Opto-Electronic Advances

Original Article

2020, Vol. 3, No. 11

DOI: 10.29026/oea.2020.200001

Observation and optimization of 2 μm mode-locked pulses in all-fiber net anomalous dispersion laser cavity

Wanzhuo Ma[1,2], Desheng Zhao[1,2], Runmin Liu[1,2], Tianshu Wang[1,2]*, Quan Yuan[1,2], Hao Xiong[1,2], Haiying Ji[1,2] and Huilin Jiang[1,2]

We integrally demonstrate 2 μm mode-locked pulses performances in all-fiber net anomalous dispersion cavity. Stable mode-locking operations with the center wavelength around 1950–1980 nm can be achieved by using the nonlinear polarization rotation structure and properly designing the dispersion management component. Conventional soliton is firstly obtained with a total anomalous dispersion cavity. Due to the contribution of commercial ultra-high numerical aperture fibers, net dispersion is reduced to -0.077 ps^2. So that stretched pulse with 19.4 nm optical bandwidth is obtained and the de-chirped pulse-width can reach 312 fs using extra-cavity compression. Under pump power greater than 890 mW, stretched pulse can evolve into noise-like pulse with 41.3 nm bandwidth. The envelope and peak of such broadband pulse can be compressed with up to 2.2 ps and 145 fs, respectively. The single pulse energy of largely chirped stretched and noise-like pulse can reach 1.785 nJ and 1.53 nJ, respectively. Furthermore, extra-cavity compression can also contribute to a significant increase of peak power.

Keywords: fiber lasers; mode-locked lasers; 2 μm fiber lasers

Ma W Z, Zhao D S, Liu R M, Wang T S, Yuan Q et al. Observation and optimization of 2 μm mode-locked pulses in all-fiber net anomalous dispersion laser cavity. *Opto-Electron Adv* **3**, 200001 (2020).

Introduction

The 2 μm fiber lasers have become the research focus because of its irreplaceable function in various fields such as laser medicine, LiDAR, gas detection, mid-IR optical parametric oscillator (OPO), free-space optical communication and supercontinuum generation[1–6]. Similar to fiber lasers at 1 μm and 1.55 μm band, the realization of ultrashort and high energy pulses at 2 μm band is of great importance in the fields of material processing and free space transmission. Various classical and emerging mode-locked structures such as nonlinear polarization rotation components[7,8], nonlinear amplifier loop mirrors[9,10], multimode interference structures[11,12], actively mode-locking components[13] and two dimensional material saturable absorbers[14,15] can be used to generate 2 μm ultra-short pulses in thulium or holmium doped fiber lasers.

Theoretically, there is little difference in mode-locked mechanisms between 2 μm and other conventional band fiber lasers. However, at present there is still a major gap between 2 μm mode-locked fiber lasers and 1.55 μm fiber lasers in pulse-width, pulse-energy, repetition rate and other parameters. The main restriction is the strong anomalous group velocity dispersion (GVD) and transmission loss of commercial silica fibers 2 μm band. It increases the difficulties of generating various types of high-energy mode-locked pulses such as dissipative

[1]National and Local Joint Engineering Research Center of Space Optoelectronics Technology, Changchun University of Science and Technology, Changchun 130022, China. [2]College of Opto-Electronic Engineering, Changchun University of Science and Technology, Changchun 130022, China.

*Correspondence: T S Wang, E-mail: wangts@cust.edu.cn

Received: 2 January 2020; Accepted: 19 February 2020; Published: 27 November 2020

solitons, noise-like and dissipative soliton resonance pulses. It also results in the restrictions of compressing mode-locked pulses with all-fiber structures. An intuitive solution is to use bulk extra-cavity structure consisted of grating pairs. It can achieve 2 μm mode-locked pulses with average power greater than 1 kW and pulse-widths of 265 fs[16]. Similarly, bulk Martinez compressor has been applied as dispersion management component in 2 μm mode-locked fiber lasers so that higher pulse energy can be achieved[17–19]. However, due to its complex structure, it relies heavily on environmental stability, which makes it difficult to be applied in practical optical systems.

By using all-fiber dispersion management devices, the sensitivity and stability against free-space bulk structure can be further improved. It can be applied effectively in both pulse compression and intra-cavity dispersion management. By properly designing the net dispersion and nonlinearity in cavity, superior mode-locked states such as stretched pulse[20], dissipative soliton[21], self-similar pulse[22] and noise-like pulse[23] can be obtained. There are several methods to move the zero dispersion point to longer wavelength such as using novel materials instead of silica, fabricating chirped Bragg grating, changing numerical aperture or core diameter. The third method has obvious advantages in cost and practicability. Further, a significant discovery in recent years is that several commercial ultra-high numerical aperture (UHNA) fibers exhibit positive GVD at the 2 μm band. In 2011, it is confirmed by experiments in bulk structure for the first time, and 470 fs, 0.4 nJ, 2 μm mode-locked pulses in normal dispersion region[24] have been successfully realized. Soon after, dissipative soliton and noise like pulse at 2 μm band can be generated in all-fiber cavity using the UHNA fiber as intra-cavity dispersion management component and single-wall carbon nanotubes as saturable absorber[21]. So far, there have been extensive reports on 2 μm all fiber mode-locked lasers using the UHNA fiber as dispersion management component, consequently leading to significant improvements on both pulse-width and pulse energy[21,25–28]. Nevertheless, through our previous research, we find that besides the cavity shapes, the output characteristics of the generated 2 μm mode-locked pulses are particularly sensitive to the feature and distribution of the UHNA fiber. It affects both intra-cavity dispersion and dynamics. Consequently, it is meaningful and intriguing to systematically and integrally investigate 2 μm mode-locked pulses with the all-fiber dispersion management cavity using UHNA fibers.

In this work, we demonstrate several 2 μm mode-locked pulses and their performances in all-fiber net anomalous dispersion fiber lasers. By reducing net dispersion to -0.077 ps^2 using commercial UHNA4 fibers, stretched pulse with 19.4 nm optical bandwidth is obtained and the de-chirped pulse-width can reach 312 fs using extra-cavity compression. By increasing pump power to 890 mW, stretched pulse can evolve into noise-like pulse with a much broader bandwidth up to 41.3 nm. The envelope and peak of such broadband pulse can be compressed to 2.2 ps and 145 fs respectively. The pulse energy and peak power of the proposed two pulses, together with small chirped stretched pulse are fully discussed.

Experimental setup and operation principles

The experimental setup of the proposed all-fiber thulium-doped mode-locked fiber laser is shown in Fig. 1. The whole laser structure consists of three subcomponents: mode-locked laser cavity, extra-cavity compression component, and subsequent amplifier, respectively. The mode-locked laser employs a conventional fiber ring cavity. A commercial laser diode combining with an Erbium-doped fiber amplifier (EDFA) is used as pump source. The center wavelength of pump laser locates at C band and the maximum output power is 1 W. A segment of 16 cm high thulium-doped fiber (TDF1 SM-TSF-5/ 125) is used as gain medium, which is pumped by the C band laser through a 1550/1900 wavelength division multiplexer (WDM). The GVDs of single-mode fiber and highly-doped TDF are -0.085 ps^2/ m and -0.051 ps^2/ m, respectively. A classic nonlinear polarization rotation (NPR) structure consisting of a polarization-dependent isolator (PD-ISO) and two squeezed polarization controllers (PC) is used to realize mode-locking operation. Additional single-mode fiber or UHNA fibers with customized length are spliced in cavity to control the nonlinearity and net dispersion respectively. The mode-locked pulses are compressed outside the cavity. The output pulses are firstly injected into a segment of the UNHA fiber, and then amplified by a homebuilt master oscillator power amplifier to meet the detection condition of autocorrelator (FR-103XL). In order to avoid the fusing of the splicing point under high power pump, the gain medium in amplifier is selected as 3.5 m TDF2 (SM-TSF-9/125) with GVD of -0.088 ps^2/ m. Note that the length of UHNA fiber is specially designed to compensate both the intra-cavity and extra-cavity

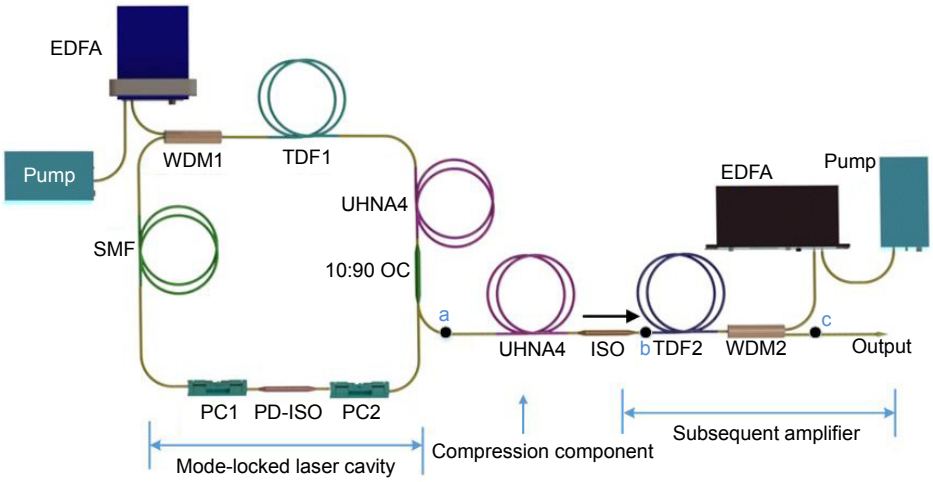

Fig. 1 | Experimental set-up of dispersion-managed mode-locked thulium-doped fiber laser.

anomalous dispersion induced by amplifier. In addition, the place of the UHNA fiber is of vital significance because its broadening effect on pulses can avoid the distortion due to nonlinear effects caused by high peak power during power amplification. If the UHNA fiber is spliced after amplifier, the distortion of autocorrelation trace will be noticeable due to the high nonlinearity of UHNA fiber. The output spectrum can be observed by an optical spectrum analyzer (OSA, Yokogawa AQ6375). The pulses are detected by a 2 μm InGaAs PIN photo-detector with 12 GHz bandwidth and 28 ps rising time. The RF pulse is observed by an oscilloscope (Agilent, DSO9254A) with the bandwidth of 2.5 GHz. The RF spectrum is measured by a radio frequency spectrum analyzer (Agilent, N1996A).

Nonlinearity and dispersion in cavity are the key elements to determine the mode-locked pulse dynamics. By virtue of nonlinearity, the SMF length is properly set to meet the requirements of high stability and spontaneous mode-locking operations. The normal dispersion characteristics at 2 μm band of the UHNA fibers are attributed to their specific waveguide dispersion which is altered by drastically increasing the numerical aperture (NA) and decreasing the radius. The parameters of three commercial UHNA fibers from Nufern company are shown in Table 1. It should be noted that the GVD value of UHNA fibers are scarce and inconsistent in some of the previous reports[21,29]. Herein we followed the GVD values of UHNA4, UHNA7 and SM2000D fibers measured by improved spectral interferometry technique[30]. Another notable feature here is that the mismatch of NA and radius between the UHNA fibers and SMF will lead to a considerable splicing loss. Considering both loss and dispersion value, UHNA4 fiber has presented best practicability in our experiments.

Results and discussions

To start with, the mode-locked laser firstly operates without any dispersion-management component. By gradually increasing pump power to 232 mW, conventional soliton can be obtained by setting the cavity length as 6.04 m, which only consists of SMF pigtails, additional 3.06 m SMFs and 0.16 m TDF. The net dispersion is about -0.508 ps^2. The center wavelength of soliton spectrum locates at 1980 nm. It contains symmetrical Kelly sidebands on both sides and the 3 dB bandwidth is about 8 nm, as shown in Fig. 2(a). The pulse train is shown in Fig. 2(b) and one can see the pulse interval is about 30.3 ns, indicating the round trip time of soliton in cavity. The autocorrelation trace is measured by directly injecting

Table 1 | Parameters of commercial UHNA fibers.

Fiber	NA	Radius (μm)	β2 (ps^2/m)
UHNA4	0.35	2.2	+0.091
UHNA7	0.41	2.4	+0.046
SM2000D	0.37	2.1	+0.137

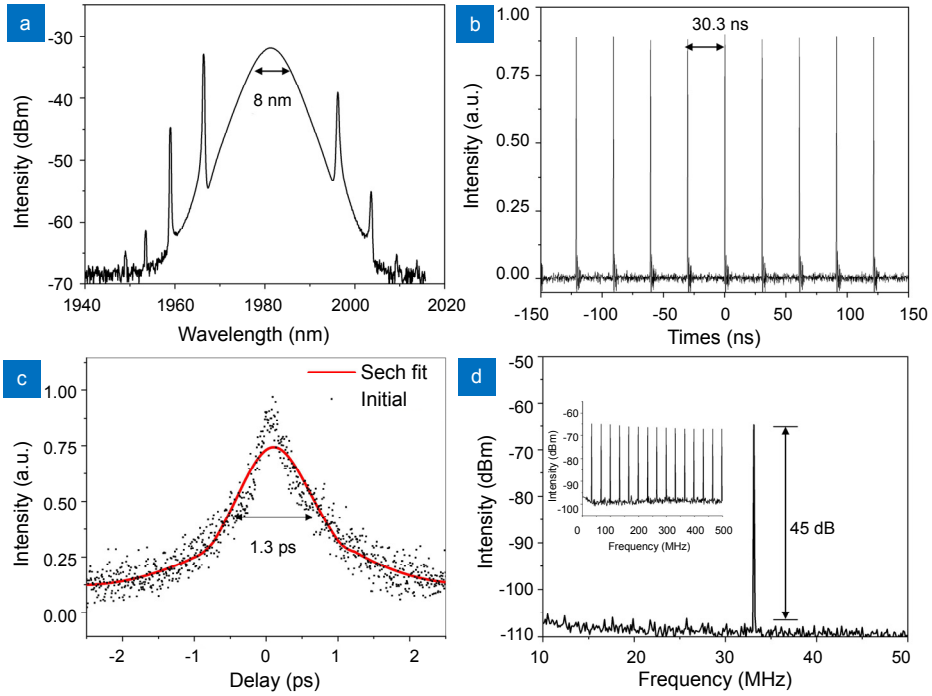

Fig. 2 | Conventional soliton at -0.508 ps^2 net dispersion. (**a**) Optical spectrum. (**b**) Pulse train. (**c**) Autocorrelation trace. (**d**) RF spectra.

soliton pulses into the subsequent amplifier, and the average output power is increased up to 50 mW to meet the detection conditions of autocorrelator. The initial autocorrelation trace and its hyperbolic secant fitting profile are shown as Fig. 2(c), indicating that the pulse-width is 1.3 ps. The corresponding time-bandwidth product (TBP) is 0.796. The difference value between the output pulse and Fourier transform limit pulse is caused by both extra-cavity dispersion and nonlinearity during amplification. In addition, as the initial output power is lower than 2 mW, the background noises induced by amplifier also partly contribute to the distortion of autocorrelation trace. This problem can be improved by replacing the detector with a more sensitive one in autocorrelator or employing a commercial low-noise amplifier. Figure 2(d) shows the RF spectra with a fundamental repetition rate of 33 MHz and the side mode suppression ratio (SMSR) is about 45 dB. Both SMNR and the frequency comb spectrum (insert) indicate a good stability.

Based on the realization of soliton pulse, the composition of cavity is readjusted. A segment of 2.9 m UHNA4 fiber is spliced between TDF and OC. The total cavity length is 6.98 m with -0.077 ps^2 net dispersion. Mode-locked operation can be achieved with pump power greater than 500 mW. The alternating dispersion components in cavity can result in a proportional reduction of continuous wave. Dispersion management also plays a key role in avoiding excessive accumulation of nonlinear phase shifts, so that the optical spectra become broader and smoother. Herein, compared with conventional soliton at -0.508 ps^2 net dispersion, the pulse with dispersion management has its net dispersion precisely decreased and it leads to a broadening of optical spectrum up to 19.4 nm, as shown in Fig. 3(a). As there is little difference between normal and anomalous dispersion in value, mode-locked pulse is periodically compressed and broadened in cavity. Consequently, the peak power can be reduced and it leads to a higher splitting threshold. Due to this process, mode-locked pulse can still keep stable fundamental frequency operation when pump is increased to the maximum power of 1 W. The round trip time of stretched pulses is 33.9 ns (see Fig. 3(b)) and the SMSR of RF spectra remains around 50 dB (see Fig. 3(c)). The mode-locked pulse is largely chirped because of the alternating dispersion, which can be visually observed by autocorrelation trace and its Gauss fitting profile as shown in Fig. 3 (d). The initial pulse-width is 4.91 ps corresponding to the TBP of 7.29, which is far greater than limiting value, indicating a large space for compression. We also use UHNA4 fiber to compress the stretched pulse outside the cavity. Considering that the amplifier has induced anomalous dispersion of 0.648 ps^2, the UHNA length in compressor is selected to be 7.5 m. The compressed autocorrelation trace with 312 fs

minimum pulse-width is shown in Fig. 3(e). The corresponding TBP is only 0.463, indicating a good compression process. In addition to the narrower pulse-width, another advantage is the tolerance to high pump power. Once the PC state is fixed, stretched pulse can maintain fundamental frequency operation even with maximum pump power of 1 W, and this feature will be further discussed in the subsequent section.

On the basis of stretched pulse operation, when pump power is further increased to 890 mW and PC is carefully adjusted, an interesting phenomenon occurs that the spectrum is suddenly broadened to about 30 nm, and there is a continuous light component in the spectrum, as shown in Fig. 4(a). The continuous light component can be gradually suppressed by constantly optimizing the PC state. As a result of this evolution, the whole spectrum becomes smoother and broader with up to 41.3 nm bandwidth, as shown in Figs. 4(b–d). The profiles of optical spectra keep close to the original one while the pump power is gradually increased to 1 W, as shown in Fig. 4(e). The obtained mode-locked pulse keeps stable fundamental frequency operation during this process which is similar to stretched pulse in Fig. 3 and the SMSR of RF spectra remain around 46 dB which is shown as Fig. 4(f). By fixing pump power at 890 mW, the autocorrelation trace is shown in Fig. 4(g). One can see that the autocorrelation trace has a large base and there is a distinct peak with pulse width on femtosecond level around the center location. Based on the performance of autocorrelation trace and optical spectrum, the newly generated mode-locked pulse can be determined as noise-like pulse at anomalous dispersion region with dispersion-managed cavity which is due to the soliton collapse effect[31,32]. Depending on the linear cavity phase delay, soliton can be switched into noise-like pulse with an appropriate cavity position and pump power[31]. The noise like pulse is essentially a pulse envelope composed of multiple ultrashort pulses with randomly varying width and peak power within a certain range. Consequently, to investigate the pulse with performance, the autocorrelation traces obtained here are averagely sampled with 256 times. One can see the original base width is about 9.7 ps corresponding to the pulse envelope width. Zooming in at the peak signal, one can see the average peak width is 539 fs as shown in Fig. 4(h) and the estimated TBP is 1.6. It has been confirmed in previous simulation studies the 3 dB duration of coherent peak corresponds to the average width of the ultrashort pulses in the envelope. The multi-pulses can also be de-chirped using extra-cavity compressor, and the duration of coherent peak after compression is only 145 fs as shown in Fig. 4(j). The corresponding TBP is 0.459. Another interesting observation

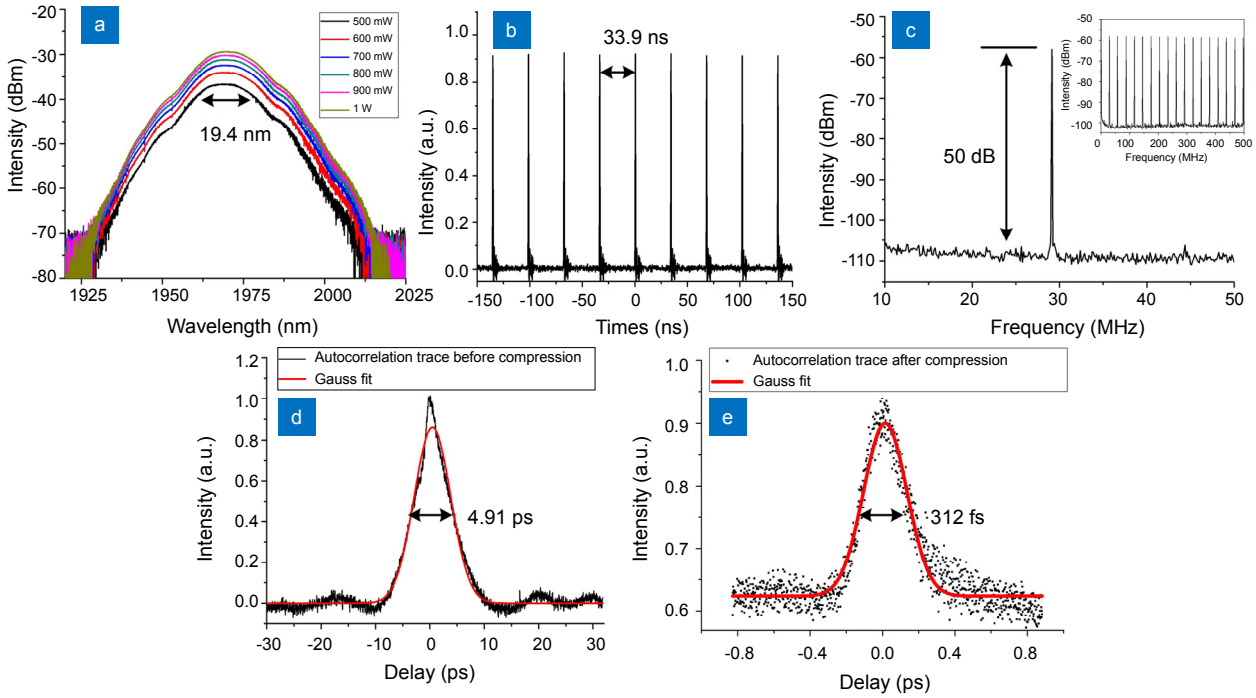

Fig. 3 | Gaussian-type stretched pulses at -0.077 ps^2 net dispersion. (**a**) Gaussian-type spectra. (**b**) Pulse train. (**c**) Radio frequency spectra. (**d**) Autocorrelation trace before compression. (**e**) Autocorrelation trace after compression.

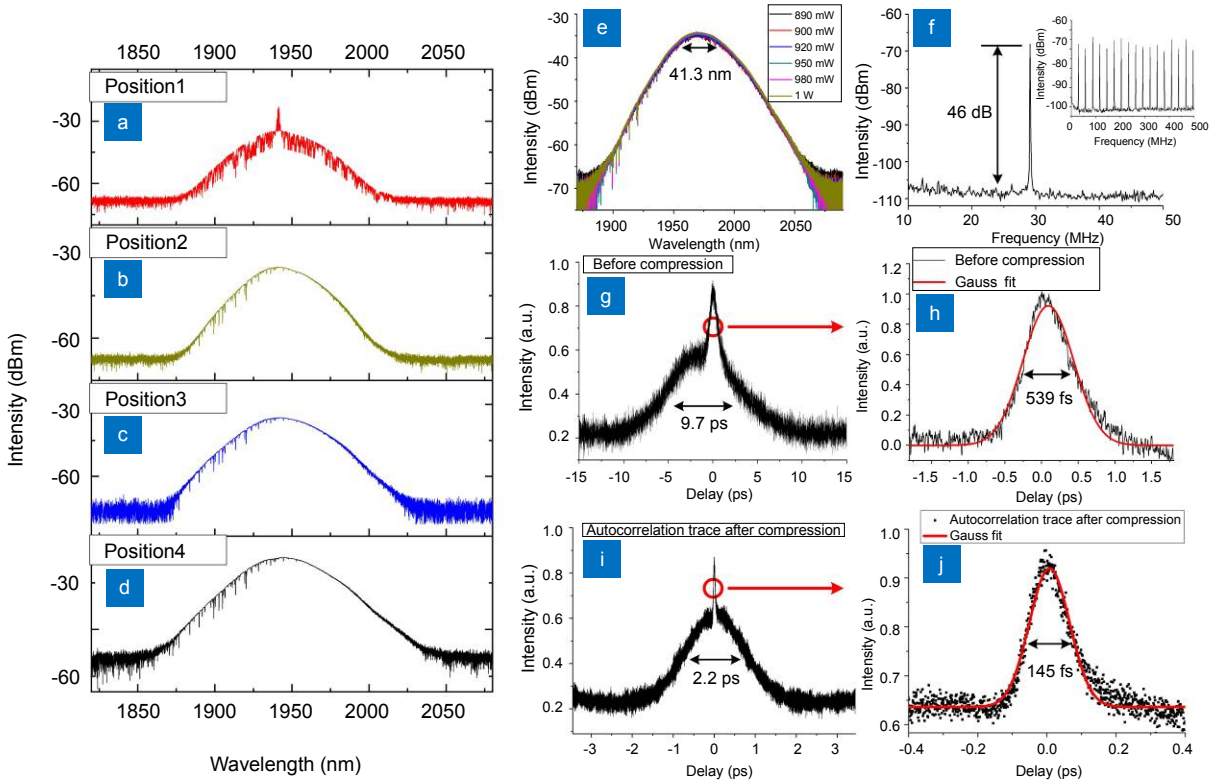

Fig. 4 | Performance of noise-like pulses. (**a**)–(**d**) Spectra evolution process of noise-like pulse. (**e**) Spectra with different pump power. (**f**) RF spectra. (**g**) Integrated autocorrelation trace before compression. (**h**) Peak autocorrelation trace before compression (at point a in Fig. 1). (**i**) Integrated autocorrelation trace after compression (at point c in Fig. 1). (**j**) Peak autocorrelation trace after compression (at point c in Fig. 1).

is that the envelope width after compression is also decreased to 2.2 ps as shown in Fig. 4(i). We deduce that it is because multi-pulses in envelope have different group velocities during the transmission outside the cavity, so that the average interval between adjacent sub-pulses is reduced.

The scheme has shown superior performance of mode-locked pulses evolution and optimization. However, in the experiment, UHNA4 fiber always causes an inescapable insertion loss which contains both splicing and transmission loss. In order to estimate the specific values of the above two losses, both ends of the UHNA4 fiber with different lengths are spliced to SMFs, as shown in Fig. 5. The input and output power are measured by power meter (Thorlabs S302C) in real time. Herein the splicing loss is approximately considered as constant by keeping the readings on welding fusion splicer at 0.02 dB, and the transmission loss of 0.4 m SMF is ignored. Thereby the splicing and transmission loss can be calculated by testing the total loss with 5 m and 9 m UHNA fiber respectively. The testing and calculating results are shown in Table 2. One can see the transmission loss of the UHNA4 fiber dramatically increases from 0.026 dB/m to 0.075 dB/m as laser wavelength is shifted from 1550 nm to 1980 nm. Meanwhile the splicing loss increases slightly from 0.395 dB to 0.4125 dB. Consequently, the length of UHNA fibers and their proportion to total cavity should also be noticed because of their influence to output dynamics and energy performance.

To further investigate energy and power characteristics of the proposed scheme, another smaller chirped stretched pulse with about 12 nm bandwidth is also established by only controlling the net dispersion properly. The single pulse energy without any amplification of stretched pulse with small chirp, stretched pulse with large chirp in Fig. 3, and noise-like pulse in Fig. 4 is presented in Fig. 6(a). One can see slightly chirped stretched pulse presents the highest single pulse energy in the pump power range of 550 mW–690 mW and it reach 1.38 nJ when pump power is 690 mW. However, it is difficult to keep fundamental frequency operation at higher pump power. For largely chirped stretched pulse, it can maintain stable fundamental frequency operation in the pump power range of 500 mW–1 W and the maximum single pulse energy can reach 1.785 nJ. The noise like pulse can only be generated under high pump power (890 mw–1 W) and the maximum single pulse energy is 1.53 nJ. It should be noted that the energy of

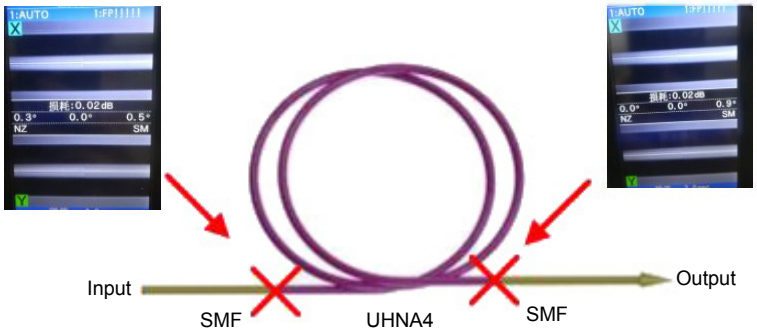

Fig 5 | Schematic diagram of UHNA4 fiber loss measurement.

Table 2 | Testing results of insertion loss.

Wavelength (nm)	1550	1980
Input power (dBm)	10	10
Total loss with 5m UHNA4 fiber (dB)	0.92	1.2
Total loss with 9m UHNA4 fiber (dB)	1.024	1.5
Estimated transmission loss (dB/m)	0.026	0.075
Estimated splicing loss per point (dB)	0.395	0.4125

largely chirped stretched pulse and noise like pulse will be further enhanced with the increase of pump power. Multi-pulse phenomenon will also occur when they exceed their respective splitting thresholds. The energy of three pulses has been increased by an order of magnitude comparing with conventional soliton in Fig. 2. The peak power of the three types of pulses as a function of pump power is shown in Fig. 6(b). One can see the maximum peak power of proposed three pulses without any compression is 1.46 kW, 0.36 kW and 0.162 kW respectively. Considering the insertion losses of UHNA4 fibers, the corresponding peak power after compression can be changed to 1.9 kW, 2.94 kW and 0.49 kW respectively (Fig. 6(c)), as the pulse-width of largely chirped stretched pulse and noise like pulse is greatly reduced. Similarly, the peak power of largely chirped broadening pulse and noise like pulse can be further improved by increasing the pump power within a certain range.

Conclusion

In conclusion, we have systematically and integrally discussed a series of 2 μm mode-locked pulses performances in net anomalous dispersion fiber lasers. By using UHNA fibers and properly designing the cavity, conventional soliton can be optimized to stretched pulse with 19.4 nm optical bandwidth. The de-chirped pulse-width can reach 312 fs using extra-cavity compression. In the same cavity, stretched pulse can evolve into noise-like pulse with 41.3 nm bandwidth under pump power greater than 890 mW. The envelope and peak of such broadband pulse can be compressed up to 2.2 ps and 145 fs respectively. Both stretched pulses and noise-like pulses have presented the capacity to maintain stable operation with single pulse energy greater than 1 nJ and more. On this foundation, extra-cavity compression based on UHNA fibers can also further increase peak power to kilowatt level. This work

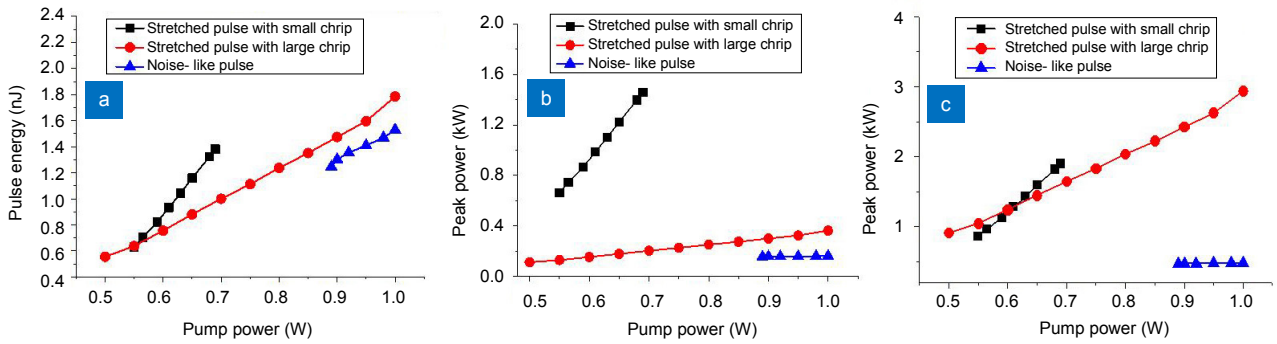

Fig. 6 | (**a**) Single pulse energy as a function of pump power. (**b**) Peak power as a function of pump power before compression (at point a in Fig. 1). (**c**) Peak power as a function of pump power after compression (at point c in Fig. 1).

has made significant improvements on the basis of previous studies and can also help further understanding 2 μm mode-locked pulses in all-fiber lasers.

References

1. Fried N M. Thulium fiber laser lithotripsy: an in vitro analysis of stone fragmentation using a modulated 110-watt thulium fiber laser at 1.94 μm. *Lasers Surg Med* **37**, 53–58 (2005).
2. Tunc B, Gulsoy M. Tm: fiber laser ablation with real-time temperature monitoring for minimizing collateral thermal damage: *ex vivo* dosimetry for ovine brain. *Lasers Surg Med* **45**, 48–56 (2013).
3. De Young R J, Barnes N P. Profiling atmospheric water vapor using a fiber laser lidar system. *Appl Opt* **49**, 562–567 (2010).
4. Leindecker N, Marandi A, Byer R L, Vodopyanov K L, Jiang J et al. Schunemann. Octave-spanning ultrafast OPO with 2.6–6.1μm instantaneous bandwidth pumped by femtosecond Tm-fiber laser. *Opt Express* **20**, 7046–7053 (2012).
5. Lin P, Wang T S, Ma W Z, Chen J D, Jiang H L. Propagation characteristics of 2.07 μm fiber laser in weak turbulence condition. *Opto-Electron Eng*, **47**, 190588 (2020)
6. Eckerle M, Kieleck C, Świderski J, Jackson S D, Mazé G et al. Actively *Q*-switched and mode-locked Tm^{3+}-doped silicate 2 *μ*m fiber laser for supercontinuum generation in fluoride fiber. *Opt Lett* **37**, 512–514 (2012).
7. Wang Q, Chen T, Zhang B, Heberle A P, Chen K P. All-fiber passively mode-locked thulium-doped fiber ring oscillator operated at solitary and noiselike modes. *Opt Lett* **36**, 3750–3752 (2011).
8. Ma W Z, Wang T S, Zhang Y, Liu P, Su Y W et al. Widely tunable 2 μm continuous-wave and mode-locked fiber laser. *Appl Opt* **56**, 3342–3346 (2017).
9. Wang X F, Peng X L, Zhang J H. Multistate passively mode-locked thulium-doped fiber laser with nonlinear amplifying loop mirror. *Appl Opt* **57**, 3410–3414 (2018).
10. Liu S, Yan F P, Zhang L N, Han W G, Bai Z Y et al. Noise-like femtosecond pulse in passively mode-locked Tm-doped NALM-based oscillator with small net anomalous dispersion. *J Opt* **18**, 015508 (2016).
11. Li H H, Wang Z K, Li C, Zhang J J, Xu S Q. Mode-locked Tm fiber laser using SMF-SIMF-GIMF-SMF fiber structure as a saturable absorber. *Opt Express* **25**, 26546–26553 (2017).
12. Li N, Liu M Y, Gao X J, Zhang L, Jia Z X et al. All-fiber widely tunable mode-locked thulium-doped laser using a curvature multimode interference filter. *Laser Phys Lett* **13**, 075103 (2016).
13. Ma W Z, Wang T Su, Wang F R, Wang C B, Zhang L et al. Tunable high repetition rate actively mode-locked fiber laser at 2 μm. *Opto-Electron Eng*, **45**, 170662(2018)
14. Yin K, Zhang B, Li L, Jiang T, Zhou X F et al. Soliton mode-locked fiber laser based on topological insulator Bi_2Te_3 nanosheets at 2 μm. *Photonics Res* **3**, 72–76 (2015).
15. Sotor J, Sobon G, Kowalczyk M, Macherzynski W, Paletko P et al. Ultrafast thulium-doped fiber laser mode locked with black phosphorus. *Opt Lett* **40**, 3885–3888 (2015).
16. Gaida C, Gebhardt M, Heuermann T, Stutzki F, Jauregui C et al. Ultrafast thulium fiber laser system emitting more than 1 kW of average power. *Opt. Lett.* **43**, 5853–5856 (2018).
17. Haxsen F, Wandt D, Morgner U, Neumann J, Kracht D. Pulse characteristics of a passively mode-locked thulium fiber laser with positive and negative cavity dispersion. *Opt Express* **18**, 18918–18988 (2010).
18. Haxsen F, Wandt D, Morgner U, Neumann J, Kracht D. Pulse energy of 151 nJ from ultrafast thulium-doped chirped-pulse fiber amplifier. *Opt Lett* **35**, 2991–2993 (2010).
19. Haxsen F, Wandt D, Morgner U, Neumann J, Kracht D. Monotonically chirped pulse evolution in an ultrashort pulse thulium-doped fiber laser. *Opt Lett* **37**, 1014–1016 (2012).
20. Wienke A, Haxsen F, Wandt D, Morgner U, Neumann J et al. Ultrafast, stretched-pulse thulium-doped fiber laser with a fiber-based dispersion management. *Opt Lett* **37**, 2466–2468 (2012).
21. Wang Q Q, Chen T, Li M S, Zhang B T, Lu Y F et al. All-fiber ultrafast thulium-doped fiber ring laser with dissipative soliton and noise-like output in normal dispersion by single-wall carbon nanotubes. *Appl Phys Lett* **103**, 011103 (2013).
22. Li H H, Liu J, Cheng Z C, Xu J, Tan F Z et al. Pulse-shaping mechanisms in passively mode-locked thulium-doped fiber lasers. *Opt Express* **23**, 6292–6303 (2015).
23. Sobon G, Sotor J, Martynkien T, Abramski K M. Ultra-broadband dissipative soliton and noise-like pulse generation from a normal dispersion mode-locked Tm-doped all-fiber laser. *Opt Express* **24**, 6156–6161 (2016).
24. Liu H, Kieu K, Lefrancois S, Renninger W H, Chong A et al. Tm fiber laser mode-locked at large normal dispersion. In *CLEO: 2011-Laser Science to Photonic Applications*, 1–2 (IEEE, 2011); http://doi.org/10.1364/CLEO_SI.2011.CMK1.
25. Sun B, Luo J Q, Zhang Y, Wang Q J, Yu X. 65-fs pulses at 2 *μ*m in a compact Tm-doped all-fiber laser by dispersion and nonliearity management. *IEEE Photonics Technol Lett* **30**, 303–306 (2018).
26. Pawliszewska M, Martynkien T, Przewłoka A, Sotor J. Dispersion-managed Ho-doped fiber laser mode-locked with a graphene saturable absorber. *Opt Lett* **43**, 38–41 (2018).
27. Kadel R, Washburn B R. An all-fiber stretched-pulse Thulium/Holmium co-doped ultrafast Laser. In *Frontiers in Optics 2013* (OSA, 2013); http://doi.org/10.1364/FIO.2013.FTh3B.5.
28. Zhao J Q, Li L, Zhao L M, Tang D Y, Shen D Y. Cavity-birefringence-dependent h-shaped pulse generation in a thulium-holmium-doped fiber laser. *Opt Lett* **43**, 247–250 (2018).
29. Kadel R, Washburn B R. Stretched-pulse and solitonic operation of an all-fiber thulium/holmium-doped fiber laser. *Appl Opt* **54**, 746–750 (2015).
30. Ciąćka P, Rampur A, Heidt A, Feurer T, Klimczak M. Dispersion measurement of ultra-high numerical aperture fibers covering thulium, holmium, and erbium emission wavelengths. *J Opt Soc Am B* **35**, 1301–1307 (2018).
31. Tang D Y, Zhao L M, Zhao B. Soliton collapse and bunched noise-like pulse generation in a passively mode-locked fiber ring laser. *Opt Express* **13**, 2289–2294 (2005).
32. Zhao L M, Tang D Y. Generation of 15-nJ bunched noise-like pulses with 93-nm bandwidth in an erbium-doped fiber ring laser. *Appl Phys B,* **83**, 553-557 (2006).

Acknowledgements

This work was supported in part by the National Natural Science Foundation of China 61975021, in part by the Science and Technology Project of Jilin Province under Grant 20170414041GH and in part by the Research Project of Jilin Provincial Education Department under Grant JJKH20181090KJ.

Competing interests

The authors declare no competing financial interests.